Expansion of Laser-Arc Hybrid Welding to Horizontal and Vertical-up Welding

Uemura, Takamori
Department of Civil and Structural Engineering, Kyushu University

Gotoh, Koji
Department of Marine Systems Engineering, Faculty of Engineering, Kyushu University

Uchino, Issei
Namura Shipbuilding Co., Ltd.

出版情報：Welding in the World, 2022-01-21. Springer
バージョン：
権利関係：

Title:

Expansion of Laser–Arc Hybrid Welding to Horizontal and Vertical-up Welding

Authors:

Takamori Uemura[1], Koji Gotoh[2], Issei Uchino[3]

1 Department of Civil and Structural Engineering
Kyushu University, 744 Motooka, Nishi-ku, Fukuoka, Japan

2 Department of Marine Systems Engineering
Kyushu University, 744 Motooka, Nishi-ku, Fukuoka, Japan
ORCID: 0000-0001-6813-4089

3 Namura Shipbuilding Co., Ltd.
5-1 Shioya, Kurogawa-cho, Imari-city, Saga prefecture, Japan

Corresponding author: Koji Gotoh; email: gotoh@nams.kyushu-u.ac.jp

Abstract

Laser-arc hybrid welding (LAHW) is an advanced welding method that combines arc welding and laser welding and can achieve deep penetration and the reduction of welding deformation compared with conventional arc welding. As with other welding techniques, it is common to target the flat position (PA) as the welding position. However, the expansion of the applicable positions enables the application of high-quality welded joints fabricated by LAHW to many welded joints in large steel structures. This study used the LAHW system with a robot manipulator to establish weldability in the horizontal position (PC) and the vertical-up position (PF) to expand the applicable range of LAHW in large steel structures. Suitable LAHW conditions for fabricating the butt-welded joint with a welding length of 1,000 mm for these positions were established through various investigations, including molten pool observation. Finally, the quality of these joints was evaluated in accordance with the Laser Arc Hybrid Welding Guidelines (ClassNK) of Nippon Kaiji Kyokai, and it was confirmed that the joints satisfy the required standards.

Keywords: Laser–Arc Hybrid Welding, Horizontal Position, Vertical-up Position

Declarations:

Funding:	Not applicable
Conflicts of interest/Competing interests:	Not applicable
Availability of data and materials:	Not applicable
Code availability:	Not applicable
Authors' contributions:	Not applicable

Acknowledgements

We would like to express our gratitude to all related parties for their cooperation in NDT and mechanical tests, and provision or preparation of test materials. This study was supported by JFE Steel Corporation through the provision of KC-550, which is a welding wire for J-STAR® Welding. We thank Edanz (https://jp.edanz.com/ac) for editing a draft of this manuscript.

1. Introduction

In the construction of a general merchant ship, thick plate of approximately 20 mm is employed, and a different welding position or process may be used at each construction stage. For example, in Japanese shipyards, the one-side submerged arc welding process is employed to fabricate the butt joints of large plates, and multi-layered welding is often required to construct the hull blocks. These welding processes need a groove with a "V" shape prepared in advance. Additionally, with these welding processes, the amount of heat input becomes excessive, and the quality of the welded joint may degrade [1][2].

Laser-arc hybrid welding (LAHW) is an advanced welding method that uses the advantages of laser welding and arc welding. It is expected that the use of this method will expand to the construction of large welded structures, such as general merchant ships, wherein thick plates are used as the main component. These thickness steel plates are often cut by thermal cutting in Japanese shipyards because the costs of plasma or gas cutting are lower than machining process. The groove shape is often alike to V-shape even though steel plate was cut into I-shape because the kerf shape in plasma or laser cutting is less perpendicular[3]. Indeed, a good kerf shape allows the root gap to be controlled and the variability to the welding process results is low[5]. However, research has attracted an attention about the kerf shape since it is possible to decrease laser power by applying less perpendicular kerf shape for welding thickness steel plates[3]-[6]. In recent years, inexpensive but high-performance laser oscillators have been developed, and the practical application of joining technology using a laser heat source for large steel structures is increasing [7]-[9]. When LAHW is applied to thick plate structures, most joints are butt joints processed in the flat position or T-joints in a fillet weld [10]-[14]. However, it is desirable to be able to use LAHW for various joint types and positions to expand the application range of the high-quality welded joints obtained by LAHW and achieve cost-effectiveness in terms of equipment installation. Studies using hybrid welding in the horizontal position (PC [15]) and vertical-up position (PF [15]) have already been conducted [16][17], but the fabrication of joints with practical lengths has not yet been achieved. In the fabrication of long joints, such as those exceeding 1 m, welding tests considering a large weld length are necessary for the practical application of hybrid welding, because thermal lensing of the laser optical system and the laser focus shift caused by the induced plume often occur under irradiation over a long time period [18].

Therefore, it is necessary to verify the weldability with this welding method against the welding procedure qualification test in PC and PF position. Additionally, the quality of this joint was evaluated through tests conducted in accordance with the Laser Arc Hybrid Welding Guidelines [19] of Nippon Kaiji Kyokai (ClassNK) to assess whether the joint satisfies the standards.

2. Experimental procedure

2.1. Materials

In this verification, the rolled steel for welded structure SM400B classified by the Japanese Industrial Standards (JIS) G 3106:2015 and high-strength steel KA36 classified by ClassNK were used as the specimens. The specimens used in each test are listed in **Table 1**. In test ID. VB2, a filler gauge (spacer) was used to keep the gap in the groove of all weld lines at about 1 mm, on the other hand, the groove gap in other tests were natural gap without a filler gauge. In the horizontal position, a special solid wire (JIS Z 3312: YGW18), which can achieve low spatter by spray transition in carbon dioxide gas arc welding called J-STAR® welding [20], was used. Moreover, a flux-cored wire (JIS Z 3313: T49J 0 T1-1 C A-U) was also adopted because it can easily realize straight weaving in the vertical-up position. Additionally, a backing sheet was used to fabricate one of the butt joints in the vertical-up position.

The chemical compositions and mechanical properties of the material of the specimens and weld wire are listed in **Table 2** and **Table 3**. All specimens were cleaned using a hand grinder or wire brush to completely remove the anti-rust oil and oxygen film by thermal cutting.

Table 1. Welding conditions in horizontal and vertical-up position.

Test ID	HB1	HB2	VB1	VB2
Thickness [mm]	12	16	12	12
Grade of specimen	SM400B	KA36	SM400B	SM400B
Groove shape	I shape	I shape	I shape	I shape
Cutting method	Plasma	Laser	Plasma	Machine
Groove gap [mm]	Approx. 0.0	Approx. 0.0	Approx. 0.0	Approx. 1.0
Arc current [A]	300	300	150	200
Arc voltage [V]	26.0	26.0	20.0	24.0
Laser power [kW]	10.0	15.0	6.0	6.0
Travel speed [mm/min]	800	800	200	400
Leading heat source	Arc	Arc	Laser	Arc
Backing sheet	None	None	Used	None

Table 2. Chemical compositions of applied steel plate and welding wire.

	Chemical compositions [Wt.%]					
	C	Si	Mn	P	S	Fe
SM 400B	0.11 - 0.14	0.18 - 0.22	0.95 - 1.03	0.012 - 0.016	0.003 - 0.005	Bal.
KA 36	0.14	0.28	1.17	0.016	0.005	Bal.
Solid wire	0.05	0.7	1.9	0.01	0.01	Bal.
FCW	0.05	0.55	1.28	0.014	0.009	Bal.

Table 3. Mechanical properties of applied steel plate and welding wire.

	Yield stress [MPa]	Tensile strength [MPa]	Elongation [%]
SM 400B	297 - 357	434 - 452	30 - 34
KA 36	444	536	24
Solid wire	571	621	30
FCW	490	580	26

2.2. Test procedure

This study used a LAHW system consisting of a digital inverter-controlled pulse automatic welding machine as MAG (Metal Active Gas) welding and a 20-kW Yb fiber laser. In this study, the shielded gas is pure CO_2 gas as active gas since almost Japanese shipyard used CO_2 gas for cost down. It has already been reported that LAHW can be performed using CO_2 gas [21]. The core diameter of fiber was 300 μm, the focal length was 300 mm, and the spot diameter of focal position was 0.5 mm. The special jig supporting arc torch and laser head was attached to the tip of the vertical articulated manipulator and each welding position and laser irradiation position were taught using a programming pendant. The appearance of the welding apparatus in PC and PF is shown in **Fig. 1**. Each specimen was supported at 4 (PC) or 6 (PF) points by simple clamping jig and removed when the surface temperature of specimens was almost under 60 degrees after welding.

For all joints, tack welding by laser welding was used and an end-tab piece was attached in advance. All test conditions used in this study are listed in **Table 1**.

(A) LAHW-PC (Horizontal position) **(B) LAHW-PF (Vertical-up position)**

Fig. 1. Photograph of LAHW in horizontal and vertical-up position.

3. Results and discussion

3.1. Weldability in horizontal position

Based on previous studies [17][22][23] and the technical knowledge obtained from the authors' investigations, it is concluded that laser welding or the LAHW method are suitable for fabricating butt joints in the horizontal position and that the influence of errors in the teaching work is very small. To reduce the workload on the operator in the teaching work, the margins of various conditions were investigated

under the working conditions listed in **Table 4**.

The parameters of the construction conditions were the three factors listed in **Table 4**, and each of the three levels, including the basic condition Test ID. HB1, were investigated. In the visual inspection and macroscopic test, similar results were obtained for all conditions. However, there are differences in the results for each factor. About "Defocusing distance (Factor A)", the weld bead width and reinforcement height at back weld bead are wider or higher as the defocusing distance is closer to laser's focal length (300 mm) because the laser energy density is higher as the defocusing distance is closer to laser's focal length. However, if defocusing distance is closer to laser's focal length, the melting range of the laser becomes narrower, which may cause lack of fusion. Therefore, it is better to avoid closing defocusing distance to laser's focal length easily. About "Distance between laser irradiation point and arc torch aiming point (Factor B)", the weld bead width is narrower as the distance between laser irradiation point and arc torch aiming point is narrower. This phenomenon is predicted that the sufficient melt flow to back bead was not occurred in a groove because the position of laser heat source and arc heat source was very close. The additional investigations are needed about the effect of the distance between laser irradiation point and arc torch aiming point on the back bead formation. In the weldability investigation for "Laser head angle with horizontal position (Factor C)", the lack of fusion at the back side was observed under the condition of 15° (Test ID. HB1-C2), as shown in **Fig. 3**. In this investigation, the groove shape is I-shape, therefore, if the horizontal angle of the laser head far from 0 degrees (parallel to the face of the groove), there is a risk of lack of fusion.

Table 4. Weldability test conditions in horizontal position.

	Condition factor			Results of feat. at back weld bead	
	A	B	C	Width [mm]	Height [mm]
Test ID. HB1	15.0	2.0	10.0	5.1	0.9
Test ID. HB1-A1	10.0	2.0	10.0	6.5	1.6
Test ID. HB1-A2	20.0	2.0	10.0	2.7	0.4
Test ID. HB1-B1	15.0	0.0	10.0	2.0	0.3
Test ID. HB1-B2	15.0	5.0	10.0	3.7	0.6
Test ID. HB1-C1	15.0	2.0	5.0	3.2	0.6
Test ID. HB1-C2	15.0	2.0	15.0	5.2	0.9

Notes (Refer to **Fig. 2**.)

Factor A: Defocusing distance (DD) [mm]

Factor B: Distance between laser irradiation point and arc torch aiming point (DLT) [mm]

Factor C: Laser head angle with horizontal position (LHA) [degrees]

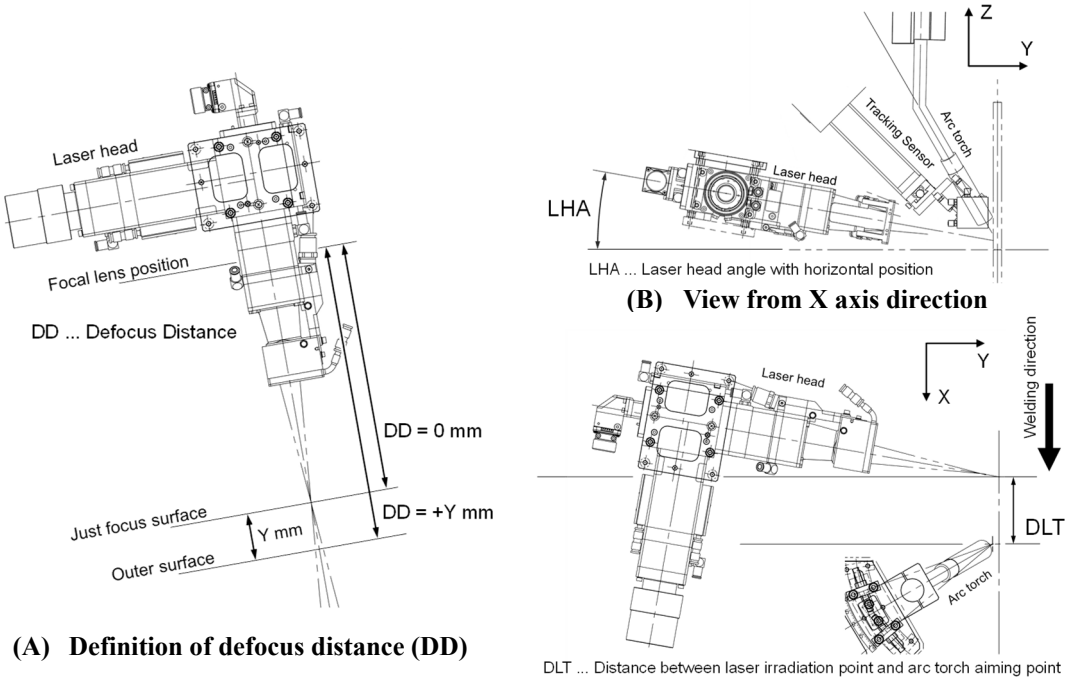

(A) Definition of defocus distance (DD)

(B) View from X axis direction

(C) View from Z axis direction

Fig. 2. Definitions each parameter in Table 4.

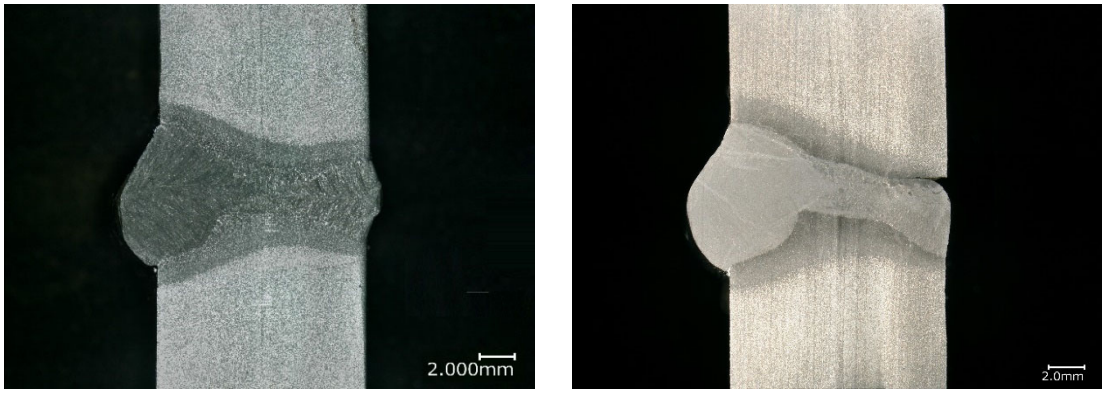

(D) Test ID. HB1 **(E) Test ID. HB1-C2**

Fig. 3. Photograph of macroscopic observation.

3.2. Weldability in vertical-up position

Generally, vertical-up welding using partly mechanized welding is a relatively difficult welding position. A flux-cored wire is often applied in the vertical-up position using MAG welding. However, few technical studies on the weldability of the vertical-up position using MAG welding with flux-cored wire have been reported. Hosoi et al. [24] reported that the mold of a slag layer supporting the molten pool is necessary to prevent molten pool dropping with partly mechanized welding, which is a phenomenon called the *mold effect*. It is assumed that this mold effect must be reproduced in LAHW. However, the molten pool dropping phenomenon is more likely to occur in LAHW, which is performed at high speed, instead of in partly mechanized welding. The mechanism and timing of this phenomenon have not been fully clarified.

Therefore, the observation of the molten pool using a high-speed camera was attempted to confirm the molten pool dropping phenomenon.

The photographs of the molten pool at the weld length points of 100 mm (30 s after the start of welding) and 280 mm (84 s after the start of welding) are shown in **Fig. 4**, when the welding conditions are based on the basic conditions listed in **Table 1**. At the welding length of 100 mm, the formation of a sufficient slag layer following the molten pool can be confirmed, but at the welding length of 280 mm, the molten metal fell down as if it had broken the slag layer. The phenomenon of molten pool dropping using flux-cored wire is unique to LAHW, because this method can achieve a large penetration depth. It is assumed that the phenomenon occurs under the following conditions:

i. When the molten pool becomes unstable owing to a change in the plume recoil pressure caused by variable changes such as changing the gap between the grooves or in laser penetration caused by the plume effect.
ii. When the amount of slag or wire supply is insufficient to achieve the *mold effect*.

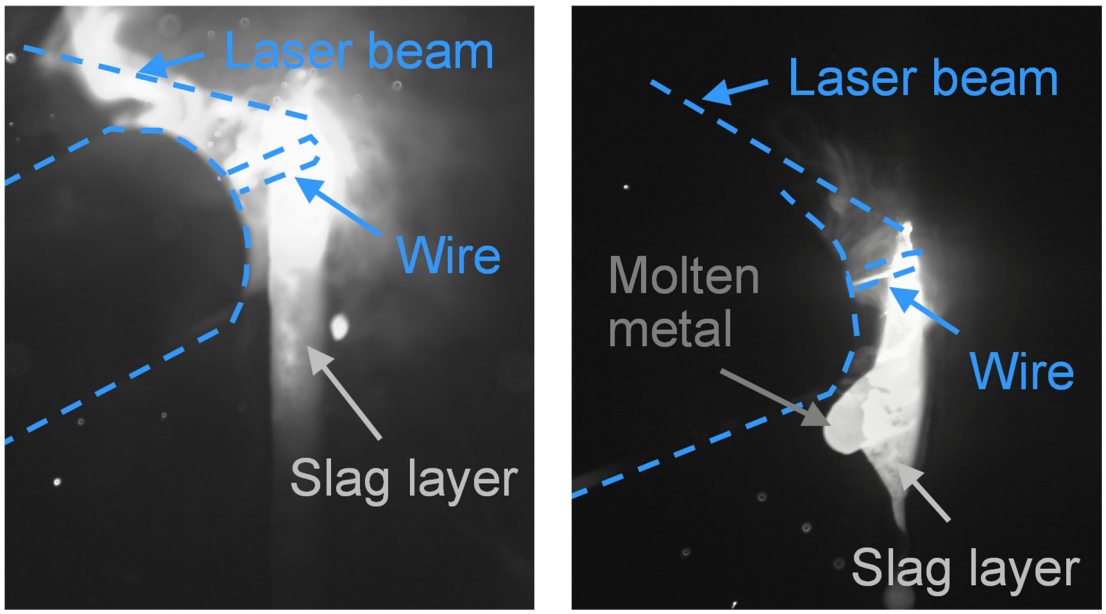

(A) At 100 mm point **(B) At 280 mm point**

Fig. 4. Molten pool formation at each weld point.

3.3. Welding procedure qualification tests

Butt weld joints with a length of 1,000 mm were fabricated under the basic conditions listed in **Table 1**, which were obtained by a preliminary investigation. The fabricated joints were inspected and tested as specified in the requirements presented in **Fig. 5** and **Table 5**.

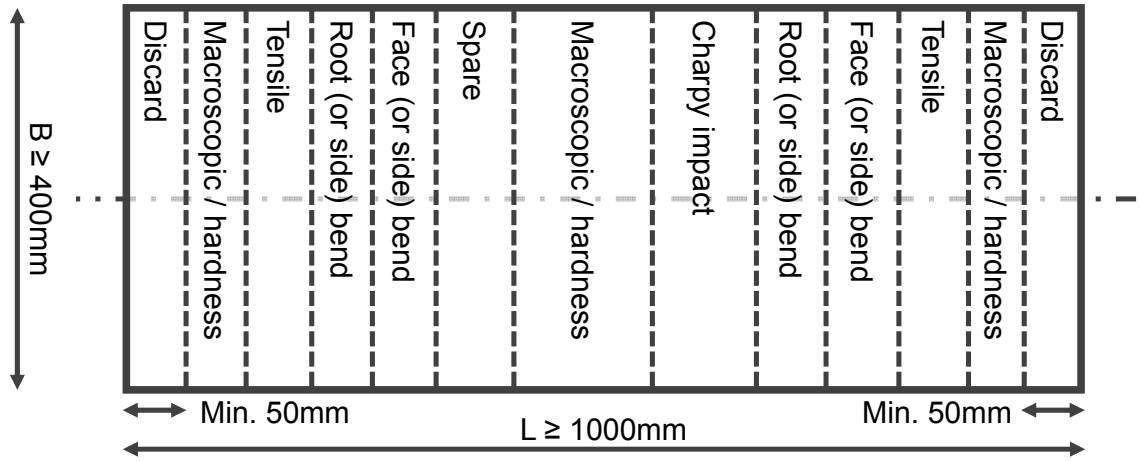

Fig. 5. Test assembly and sampling positions.

Table 5. Approval test type and requirements.

Test type	Requirements			
	Test ID HB1	Test ID HB2	Test ID VB1	Test ID VB2
Ultrasonic testing	Approval by ClassNK			
Radiographic testing	Reference: ISO 5817 Level B [25]			
Tensile test	Tensile strength [MPa]			
	≥ 400	≥ 490	≥ 400	≥ 400
Side bending test	Crack length < 3 mm			
Charpy impact test*1 *2	At center of weld metal: ≥ 23 J At fusion line (F.L.): ≥ 18 J At HAZ, 2 mm from F.L.: ≥ 18 J			
	Testing temperature [Celsius degrees]			
	0	20	0	0
Macroscopic test	No obvious defects			
Vickers hardness test	Maximum hardness ≤ 380 HV			

*1 Specimens for testing were extracted at 5-6 mm from front surface in the thickness.

*2 The test specimens were processed with side groove according to guideline published by ClassNK.

Some photographs showing the appearance of the weld bead are shown in **Fig. 6** and **Fig. 7**. It was confirmed that the bead height and width of each joint were approximately constant and stable. However, the volume of weld bead is not the same as test ID VB1 and VB2 since it is concerned that test ID VB1 was applied backing sheet and the spatters were not emitted from back side. The results of the non-destructive tests (NDT) and mechanical tests listed in **Table 5** are presented in **Table 6** to **Table 10**. In the Vickers hardness test, the test force was 1 kgf and the loading time was 15 s.

The results obtained by test ID VB1 confirm that the ultrasonic testing and Charpy impact testing did not pass the required criteria specified in the guidelines. The fracture surface of test ID VB1 at center of weld metal showed an overall brittle surface, as shown photograph **(B)** in **Table 9**. In the radiographic testing, the shadow shown in **Fig. 8** was observed over the entire weld line in the X-film, and it is assumed that this shadow was detected as a defect echo in the ultrasonic test. These shadows are traces on the surface of the back bead shown in **Fig. 9(A)**, and it is assumed that these traces are vapor routes sublimated from the backing sheet irradiated by the laser beam that penetrated the steel plate. The overall low toughness of test ID VB1 is partly attributed to the fact that the various chemical components of the backing sheet may have mixed with the molten pool consisting of the filler material and base metal, in accordance with the mechanism shown in **Fig. 9(B)**. The validity of this hypothesis requires further investigation, such as the analysis of the material composition.

For test ID VB2, cracks of up to 1.5 mm were observed in the side bending test, as presented in **Table 8** and **Fig. 10(A)**. However, as shown in **Fig. 10(B)**, the results for the joint obtained by two macroscopic tests reveal that a critical internal defect did not exist in the molten part, and this joint passed the ultrasonic test and radiographic test.

Front bead appearance

Back bead appearance

(A) Condition of test ID HB1 at 700 mm point.

Front bead appearance

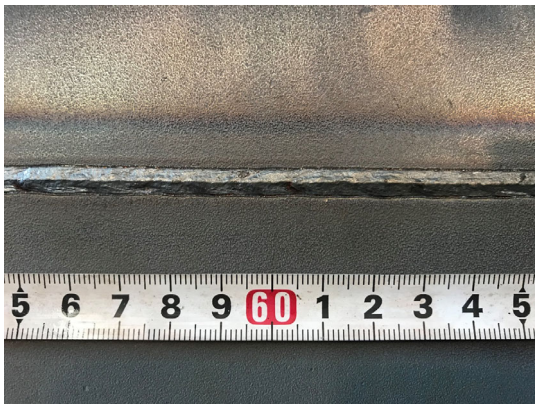

Back bead appearance

(B) Condition of test ID HB2 at 600 mm point.

Fig. 6. Photographs of weld bead appearance in horizontal position.

Front bead appearance

Back bead appearance

(A) Condition of test ID VB1 at 600 mm.

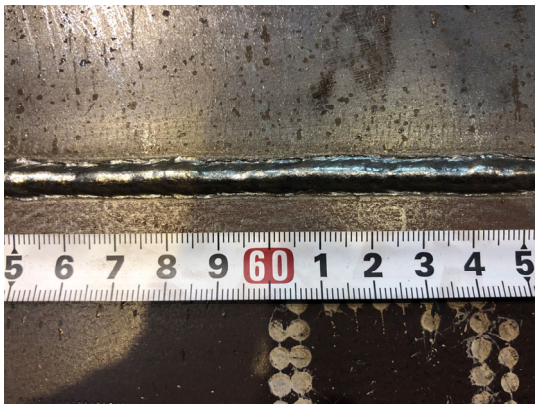

Front bead appearance

Back bead appearance

(B) Condition of test ID VB2 at 600 mm.

Fig. 7. Photographs of weld bead appearance in vertical-up position.

Table 6. Assessments by NDT.

Test ID	Ultrasonic testing	Radiographic testing
HB1	Passed	Passed
HB2	Passed	Passed
VB1	Not passed	Passed
VB2	Passed	Passed

Table 7. Results of tensile test and example of breaking appearance.

Test ID	Cross-sectional area	Tensile strength	Requirements	Breaking position
HB1	360 mm^2	464 MPa	≥ 400 MPa	Base metal
HB2	480 mm^2	552 MPa	≥ 490 MPa	Base metal
VB1	345 mm^2	496 MPa	≥ 400 MPa	Base metal
VB2	360 mm^2	464 MPa	≥ 400 MPa	Base metal

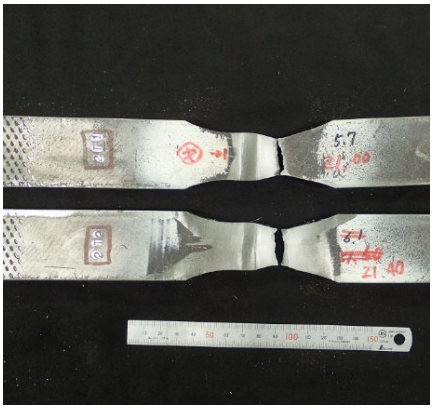

(A) Test ID HB1

(B) Test ID VB1

Table 8. Results of side bending test and example of appearances after bending test.

Test ID	Assessment or remarks (Requirement: Crack length < 3 mm)
HB1	No defect, Passed
HB2	No defect, Passed
VB1	No defect, Passed
VB2	Maximum crack length = 1.5 mm, Passed

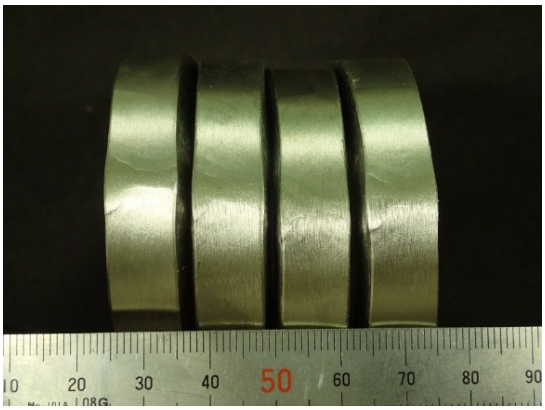

(A) Test ID HB1

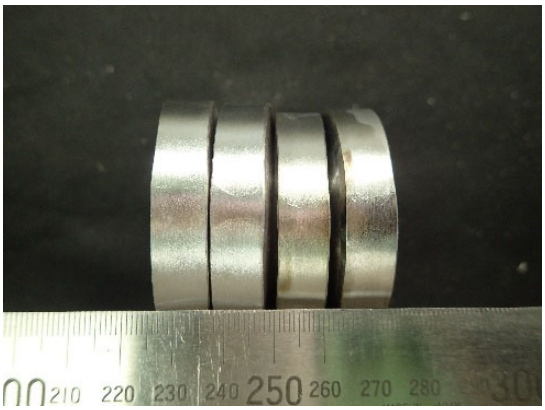

(B) Test ID VB1

Table 9. Results of Charpy impact test (minimum values) and example of fracture surface.

Test ID	At center of weld metal [J]			At fusion line (FL) [J]			At HAZ, 2 mm from FL [J]		
	N1	N2	N3	N1	N2	N3	N1	N2	N3
HB1	73	86	84	100	100	106	86	129	103
HB2	65	92	73	115	126	109	123	123	123
VB1	24	24	14*	52	15*	33	47	33	55
VB2	138	112	143	106	106	57	42	55	47
	Requirement: ≥ 23 J			Requirement: ≥ 18 J			Requirement: ≥ 18 J		

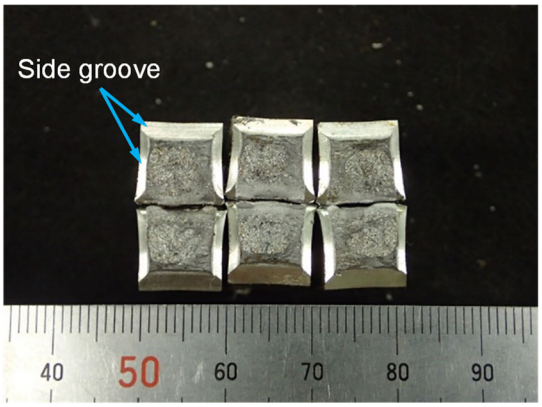

(A) Test ID HB1, At center of weld metal

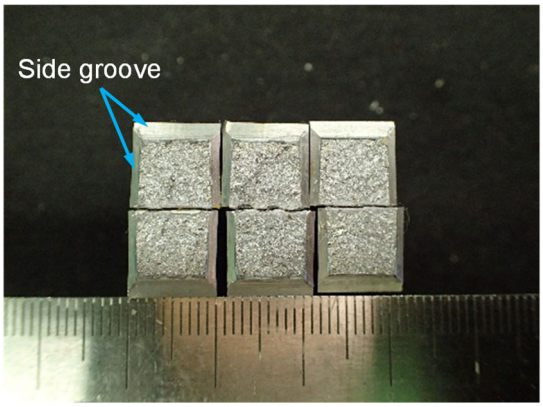

(B) Test ID VB1, At center of weld metal

* Test specimens marked with these symbols are “Not passed”.

Table 10. Results of Vickers hardness test (maximum values) and example of hardness profile.

Test ID	Position of maximum hardness point	Hardness [HV1]	Requirements
HB1	Front side in weld metal	258	≤ 380
HB2	Back side on fusion line	255	≤ 380
VB1	Back side on fusion line	216	≤ 380
VB2	Back side in weld metal	234	≤ 380

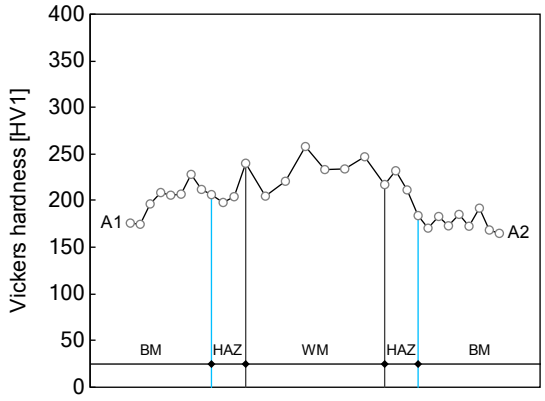

(A) Test ID HB1, At front side

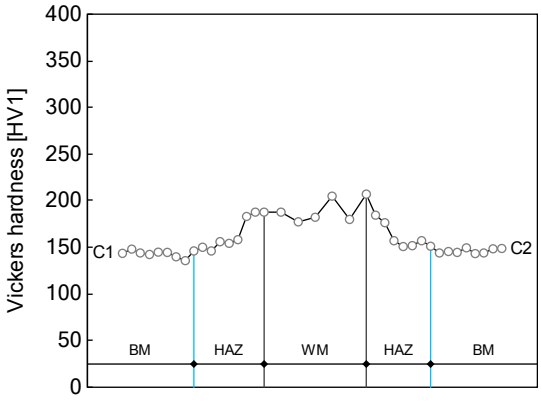

(B) Test ID VB1, At Back side

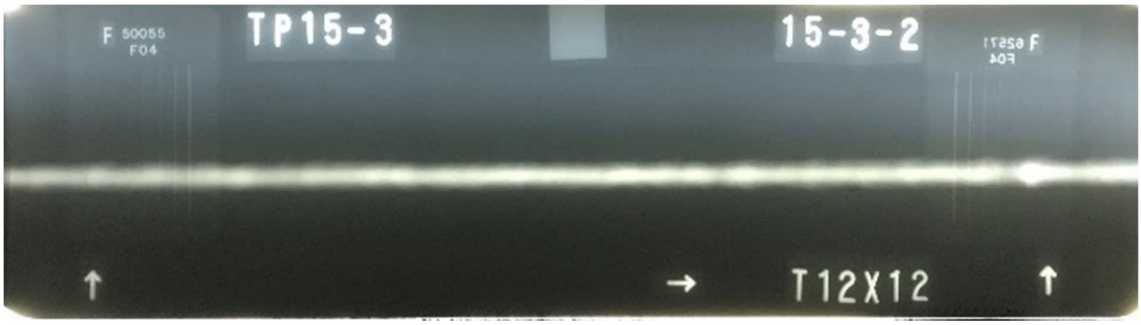

Fig. 8. Photograph of X-ray film in section of 250–500 mm in test ID VB1.

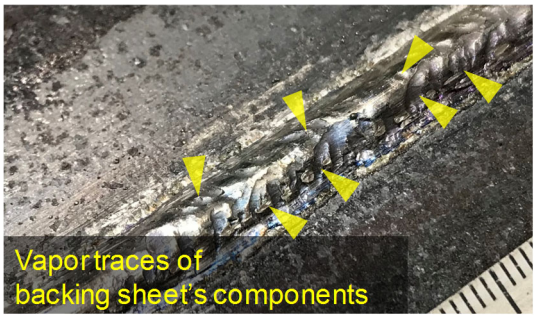

(A) Back bead appearance

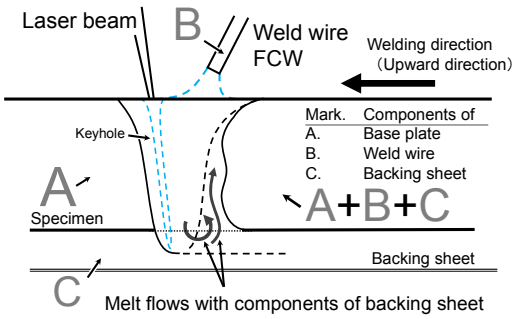

(B) Mechanism of melt flows with backing sheet

Fig. 9. Photograph of back bead appearance and schematic of melt flows in test ID VB1.

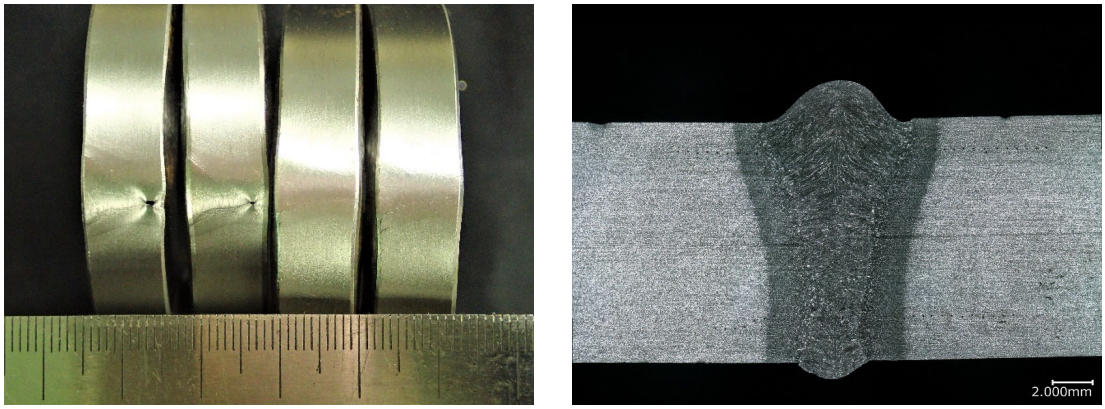

(A) Side bending test **(B) Macroscopic test**

Fig. 10. Photograph of mechanical test in test ID VB2.

4. Comparison to conventional welding

In the shipbuilding process, butt-welded joints with a thickness of approximately 12 mm are generally constructed with a horizontal or vertical-up welding position. Multilayer welding is often applied to weld a butt joint in the horizontal or vertical-up positions using semi-automatic welding. However, multilayer welding can cause angular distortion or welding deformation [26].

The welding conditions of partly mechanized welding are listed in **Table 11**. The results for the angular distortion obtained by tests ID HB1, VB1, HB MAG, and VB MAG are presented in **Table 12** and **Table 13**. Each specimen was not attached fixed jig such as strong back.

Table 11. Welding condition by partly mechanized welding.

Test ID	HB MAG	VB MAG
Arc current [A]	140 - 230	160 - 180
Arc voltage [V]	23 - 29	20 - 23
Travel speed [mm /min]	125 - 520	90 - 160
Schematic of cross-section	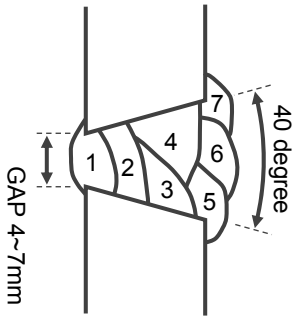	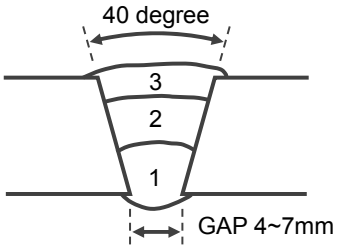
Wire type	FCW, diameter = 1.4 mm	
Shield gas type	CO_2 100%	
Groove shape	V groove, 40°	

Table 12. Angular distortion by horizontal position.

Indices at cross section Ref. **Fig. 11**	Specimen or test ID	
	HB MAG [degrees]	HB1 (LAHW) [degrees]
L6-L1-R1-R6	3.05	0.35
L7-L2-R2-R7	3.55	0.40
L8-L3-R3-R8	3.85	0.35
L9-L4-R4-R9	3.60	0.30
L10-L5-R5-R10	3.00	0.20

Table 13. Angular distortion by vertical-up position.

Indices at cross section Ref. **Fig. 11**	Specimen or test ID	
	VB MAG [degrees]	VB1 (LAHW) [degrees]
L6-L1-R1-R6	1.40	0.45
L7-L2-R2-R7	1.75	0.40
L8-L3-R3-R8	1.90	0.35
L9-L4-R4-R9	1.70	0.05
L10-L5-R5-R10	1.25	0.20

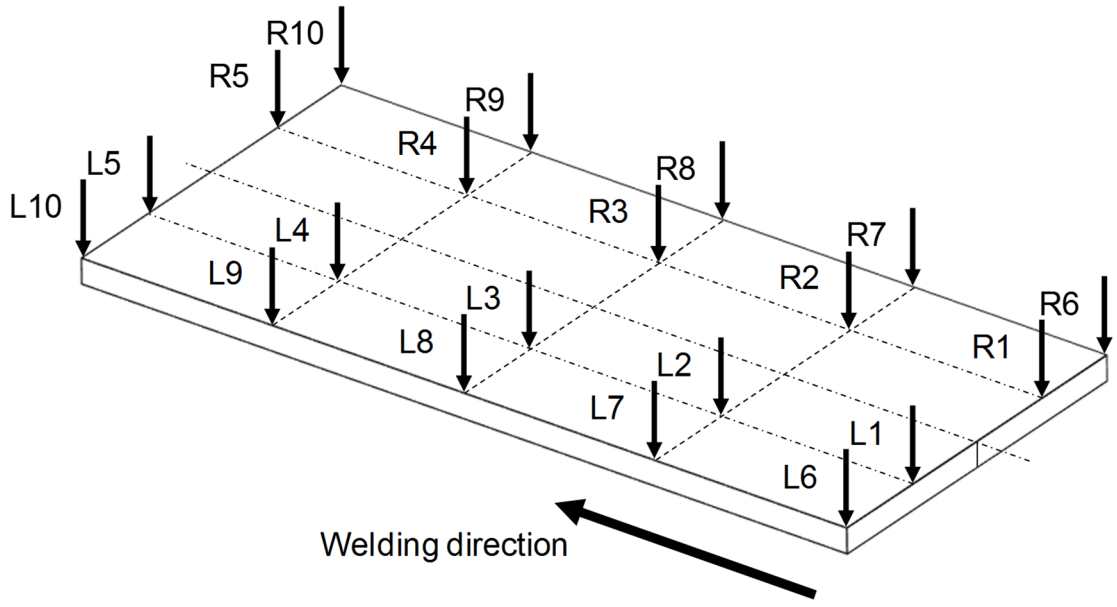

Fig. 11. Schematic of measured point and marks.

In each joint welded using partly mechanized welding, angular distortion was caused by multilayer welding and multi-run welding. In particular, the angular distortion was large in the horizontal position with many layers and welding passes. However, because LAHW can achieve one-pass and full-penetration

welding, the temperature difference between the front and back sides of the specimen tends to be smaller owing to the full penetration. Consequently, the joints have small angular distortion and welding deformation when the LAHW method is used.

5. Conclusions

This study investigated the weldability in the fabrication of butt joints using the LAHW method in the horizontal and vertical-up positions. Additionally, the weld joint quality of the joints fabricated in each welding position was evaluated based on the ClassNK guidelines. The following conclusions were drawn from this study:

(1) The weldability margins of the defocus distance, the distance between the laser irradiation point and the arc torch aiming point, and the laser head were investigated for a butt joint in the horizontal position with a plate thickness of 12 mm.

(2) The thickness of a butt joint for single-pass welding in the horizontal position with a length of 1,000 mm can be extended to 16 mm, and it is expected that the thickness can be extended further with the additional consideration of the welding conditions.

(3) Weld bead stability, avoiding dropping of the molten pool, can be obtained using a backing sheet in the fabrication of a butt joint in the vertical-up position. However, there is a risk that the laser beam penetrating the steel plate will melt the backing sheet, which will cause some of the backing sheet's components to be entrapped in the molten pool and potentially reduce the toughness of the joint.

(4) From the investigation of the dropping phenomenon of the molten pool using a high-speed camera, it is concluded that it is necessary to pay attention to the dilution ratio of the molten pool so as to obtain a sufficient amount of slag to produce the *mold effect*, and examine or select the welding conditions that maintain the balance between the amount of slag and the molten metal retained in the slag layer, particularly when attempting to fabricate a butt joint in the vertical-up position without applying a backing sheet.

(5) The butt joints fabricated under the appropriate welding conditions obtained from the preliminary investigation satisfy the requirements of the NDT and mechanical tests specified in the guidelines. The investigation of the extension of the welding position in this study can be useful for the practical application of LAHW in shipyards or elsewhere.

(6) One-pass penetration welding can be achieved by hybrid welding, and the angular deformation of each joint tends to be smaller than that of multi-layer welding by partly mechanized welding due to the smaller temperature difference caused by the welding heat input on the front and back sides of the steel plate.

Conflict of Interest

The authors declare that they have no conflict of interest.

References

[1] Lan LY, Kong XW, Qiu CL, Zhao DW (2016) Influence of microstructural aspects on impact toughness of multi-pass submerged arc welded HSLA steel joints. Mater Des 90:488-498. https://doi.org/10.1016/j.matdes.2015.10.158

[2] Shi MH, Zhang PY, Zhu FX (2014) Toughness and Microstructure of Coarse Grain Heat Affected Zone with High Heat Input Welding in Zr-bearing Low Carbon Steel. ISIJ international 54(1):188-192. https://doi.org/10.2355/isijinternational.54.188

[3] Farrokhi F, Nielsen SE, RH Schmidt et al (2015) Effect of Cut Quality on Hybrid Laser Arc Welding of Thick Section Steels. Physics Procedia 78:65-73. https://doi.org/10.1016/j.phpro.2015.11.018

[4] Farrokhi F, Kristiansen M (2016) A practical approach for increasing penetration in hybrid laser-arc welding of steel. Physics Procedia 83:577-586. https://doi.org/10.1016/j.phpro.2016.08.060

[5] Bunaziv I, Dørum C, Nielsen SE et al (2020) Laser-arc hybrid welding of 12- and 15-mm thick structural steel. Int J Adv Manuf Technol 107(5-6):2649-2669. https://doi.org/10.1007/s00170-020-05192-2

[6] Uchino I, Uemura T, Gotoh K (2021) A Study on Adopting Λ-Shape Groove for Laser-Arc Hybrid Welding to Construct Thick Plate Butt Welded Joints. Welding Int 34(7-9): 357-371. https://doi.org/10.1080/09507116.2021.1936931

[7] Graudenz M, Baur M (2013) Applications of laser welding in the automotive industry. In: Katayama S (ed) Handbook of Laser Welding Technologies. Woodhead Publishing Limited, UK, pp 555-574. https://doi.org/10.1533/9780857098771.4.555

[8] Wang H (2013) Applications of laser welding in the railway industry. In: Katayama S (ed) Handbook of Laser Welding Technologies. Woodhead Publishing Limited, UK, pp 575-595. https://doi.org/10.1533/9780857098771.4.575

[9] Reitemeyer D, Schultz V, Syassen F et al (2013) Laser welding of large scale stainless steel aircraft structures. Physics Procedia 41:106-111. https://doi.org/10.1016/j.phpro.2013.03.057

[10] Koga H, Goda H, Terada S et al (2010) First Application of Hybrid Laser-arc Welding to Commercial Ships. Mitsubishi Heavy Industries technical review 47(3):59-64.

[11] Roland F, Manzon L, Kujala P et al (2004) Advanced Joining Techniques in European Shipbuilding. Journal of Ship Production and Design 20(3):200-210.

https://doi.org/10.5957/jsp.2004.20.3.200

[12] Unt A, Salminen A (2015) Effect of welding parameters and the heat input on weld bead profile of laser welded T-joint in structural steel. J Laser Appl 27(S2):S29002. https://doi.org/10.2351/1.4906378

[13] Trichin G, Kuznetsov M, Tsibulskiy I, Firsova A (2017) Hybrid Laser-Arc Welding of the High-Strength Shipbuilding Steels: Equipment and Technology. Physics Procedia 89:156-163. https://doi.org/10.1016/j.phpro.2017.08.005

[14] Femandes CA, do Vale NL, Santos TFD, Urtiga SL (2020) Investigation of transverse shrinkage and angular distortion caused by hybrid laser-arc welding. Int J Adv Manuf Technol 107(11-12):4705-4711. https://doi.org/10.1007/s00170-020-05343-5

[15] ISO 6947 (2019) Welding and allied processes - Welding positions

[16] Chen YB, Feng JC, Li LQ et al (2013) Effects of welding positions on droplet transfer in CO2 laser-MAG hybrid welding. Int J Adv Manuf Technol 68(5-8): 1351-1359. https://doi.org/10.1007/s00170-013-4926-9

[17] Wang K, Jiao XD, Zhu JL et al (2021) Research on the effect of weld groove on the quality and stability of laser-MAG hybrid welding in horizontal position. Welding in the world. https://doi.org/10.1007/s40194-021-01125-z
Accessed 08 June 2021.

[18] Zou JL, Yang WX, Wu SK et al (2016) Effect of plume on weld penetration during high-power fiber laser welding. J Laser Appl 28(2):022003 https://doi.org/10.2351/1.4940148

[19] Nippon Kaiji Kyokai (2016) Guidelines on Laser-Arc Hybrid Welding (Ver. 3)

[20] Kataoka T, Ikeda R, Yasuda K (2007) Development of Ultra-low Spatter CO_2 Gas-shielded Arc Welding Process "J-STAR® Welding". JFE technical report 10:31-34.

[21] Wahba M, Mizutani M, Katayama S (2016) Single pass hybrid laser-arc welding of 25 mm thick square groove butt joints. Materials & Design 97:1-6. https://doi.org/10.1016/j.matdes.2016.02.041

[22] Guo W, Liu Q, Francis JA et al (2015) Comparison of laser welds in thick section S700 high-strength steel manufactured in flat (1G) and horizontal (2G) positions. CIRP annals 64(1):197-200. https://doi.org/10.1016/j.cirp.2015.04.070

[23] Sun JH, Feng K, Zhang K et al (2017) Fiber laser welding of thick AISI 304 plate in a horizontal (2G) butt joint configuration. Mater Des 118:53-65. https://doi.org/10.1016/j.matdes.2017.01.015

[24] Hosoi K, Hirata Y, Ogino Y, Kouno H (2016) MAG Welding Phenomena with Titania-Based Flux Cored Wire in Vertical Upward Position (in Japanese). Sumato Purosesu Gakkaishi (Journal of Smart Processing) 5(1):95-100.

https://doi.org/10.7791/jspmee.5.95

[25] ISO 5817 (2003) Welding - Fusion-welded joints in steel, nickel, titanium and their alloys (beam welding excluded) - Quality levels for imperfections

[26] Adamczuk PC, Machado IG, Mazzaferro JAE (2017) Methodology for predicting the angular distortion in multi-pass butt-joint welding. J Mater Process Technol 240:305-313. https://doi.org/10.1016/j.jmatprotec.2016.10.006